CrossMark

Relativistic Jets in Core-collapse Supernovae

Tsvi Piran[1] , Ehud Nakar[2], Paolo Mazzali[3,4] , and Elena Pian[5,6]

[1] Racah Institute of Physics, The Hebrew University of Jerusalem, Jerusalem 91904, Israel
[2] Raymond and Beverly Sackler School of Physics & Astronomy, Tel Aviv University, Tel Aviv 69978, Israel
[3] Astrophysics Research Institute, Liverpool John Moores University, IC2, Liverpool L3 5RF, UK
[4] Max-Planck-Institut fur Astrophysik, Karl-Schwarzschild-Str. 1, D-85748 Garching, Germany
[5] INAF, Istituto di Astrofisica Spaziale e Fisica Cosmica di Bologna, I-40129 Bologna, Italy
[6] Scuola Normale Superiore, Piazza dei Cavalieri 7, I-56126 Pisa, Italy

Abstract

After decades of extensive research the mechanism driving core-collapse supernovae (CCSNe) is still unclear. One common mechanism is a neutrino-driven outflow, but others have been proposed. Among those, a long-standing idea is that jets play an important role in supernova (SN) explosions. Gamma-ray bursts (GRBs) that accompany "hypernovae," rare and powerful CCSNe, involve relativistic jets. A GRB jet punches a hole in the stellar envelope and produces the observed gamma-rays far outside the progenitor star. While SNe and jets coexist in long GRBs (LGRBs), the relationship between the mechanisms driving the hypernova and the jet is unknown. Also unclear is the relationship between the rare hypernovae and the more common CCSNe. Here we present observational evidence that indicates that choked jets are active in CCSNe that are not associated with GRBs. A choked jet deposits all its energy in a cocoon. The cocoon eventually breaks out from the star, releasing energetic material at very high, yet sub-relativistic, velocities. This fast-moving material engulfs the star leading to a unique detectable very broad line absorption signature in early time SN spectra. We find a clear evidence for this signature in several CCSNe, all involving progenitors that have lost all, or most, of their hydrogen envelope prior to the explosion. These include CCSNe that do not harbor GRBs or any other relativistic outflows. Our findings suggest a continuum of central engine activities in different types of CCSNe and call for rethinking of the explosion mechanism of CCSNe.

Key words: gamma-ray burst: general – stars: jets – supernovae: general

1. Introduction

Massive stars end their lives in supernova (SN) explosions releasing typically $\sim 10^{51}$ erg in kinetic energy and a fraction of that in a visible light. As the star consumes its energy reservoir its core collapses and becomes a compact object. A shock wave that propagates outward ejects the envelope and synthesizes radioactive ^{56}Ni that powers part of the visible core-collapse SN (CCSN) light. So far, in addition to the explosions themselves, we have seen the massive stellar progenitors, neutrinos produced by the newborn neutron star, the compact objects left behind, and the expanding matter. All of these observations confirm the general picture outlined, already in the 1930s, by Baade & Zwicky (1934).

While the basic picture is well understood, in spite of decades of research the mechanism powering the shocks that drive the SNe is not clear. Models suggested (see e.g., Janka 2012, and references therein) include neutrino heating, magnetohydrodynamic, thermonuclear, bounce-shock, acoustic, and phase transition mechanisms. The neutrino-driven explosion, possibly in combination with hydrodynamic aspherical instabilities and non-radial flows, is the current favorite (at least for most common core collapses, SNe II), while others (e.g., bounce-shock) seem highly unlikely. Among the other mechanisms is a long-standing idea, proposed already in the early 1970s (Bisnovatyi-Kogan 1970; LeBlanc & Wilson 1970; Ostriker & Gunn 1971), that jets (particularly magnetically driven ones) play an important role in SN explosions. Here we present observational evidence for this idea.

Rare and powerful (typically 10^{52} erg) CCSNe, sometimes called hypernovae, accompany long gamma-ray bursts (LGRBs; see e.g., Woosley & Bloom 2006). These explosions involve two distinct components: a narrowly collimated relativistic jet that successfully penetrates the massive stellar envelope and produces the gamma-ray burst (GRB; see e.g., Piran 2004; Kumar & Zhang 2015, and references therein), and a more isotropic (yet not necessarily spherically symmetric) massive SN explosion. The SN ejecta typically carries ~ 10–100 times more energy than the GRB jet (see e.g., Mazzali et al. 2014, and references therein). Thus, while the jet itself cannot drive the SN explosion, it is reasonable to expect that the central rapidly rotating compact object, which must be present at the center of the collapsing star to drive the GRB jet, is related to the energy source that drives the SN explosion.

The association of SNe with GRBs brings up several important questions. First, are there hypernovae in which the GRB jets are choked within the stellar envelope and fail to break out? Second, do hidden jets exist in other types of CCSNe as well, and if so can we detect them? Finally, what is the relation, if any, between the explosion mechanism of GRB associated SNe and other types of SNe? We address these questions here. We first establish a clear observational signature of hidden jets. This signature can be detected in the early (first few days) spectra of CCSNe, provided that those arise in stars that have lost all (or almost all) of their heavy hydrogen envelopes prior to the SN explosion, namely in type Ib/c, and possibly IIb, SNe. We then proceed to demonstrate that this signature has already been observed in several SNe and that it enables us to estimate the jet parameters (its total energy and opening angle).
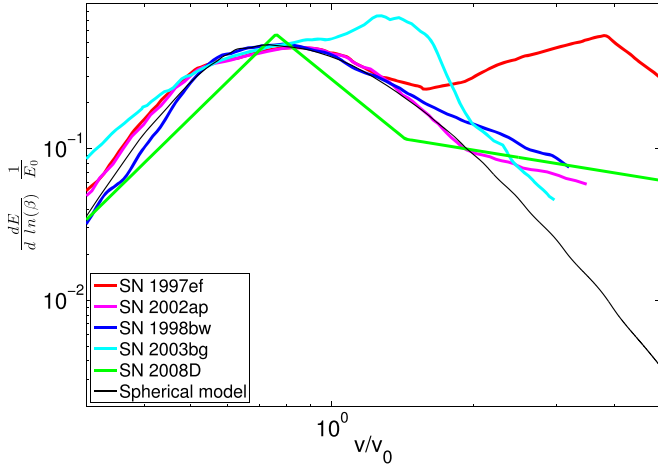
Figure 1. Energy distribution as a function of the velocity for SNe discussed here. This plot does not include SN2016jca whose distribution is similar to SN1998bw. All distributions are normalized (by v_0 and E_0) so the peaks of the distributions of the bulk of the ejecta coincide. The thin black line shows the distribution obtained from a numerical simulation, using PLUTO (Mignone et al. 2007), of a spherical explosion of a progenitor with a standard density profile near the stellar edge, $\rho(r) \propto (R_* - r)^3$, where R_* is the stellar radius. The excess of material at high velocities is naturally explained by a powerful relativistic jet that deposits all its energy in a small amount of stellar mass falling within its cocoon opening angle.

2. The Energy-velocity Profiles

As a spherical shock wave generated at the center of the collapsing star propagates outward it decelerates until it collects most of the envelope mass. At this point the shocked material velocity is $v_0 \approx \sqrt{2E_{\rm tot}/M_{\rm ej}}$, where $E_{\rm tot}$ is the total explosion energy and $M_{\rm ej}$ is the total ejected mass energy. Once the shock encounters a sharp density drop near the edge of the star it accelerates until it breaks out from the star. As the shock accelerates it loses causal contact with the energy reservoir behind it, depositing less and less energy into progressively faster and faster material. Regardless of the exact density profile near the stellar edge, the acceleration of the shock results in a rapidly decreasing energy-velocity profile of $E(v)$ with $dE/d \log(v) \propto v^{-k}$ above v_0, where $5 \leqslant k \leqslant 8$ (Matzner & McKee 1999; see Figure 1) for a typical envelop structure. $E(v)$ from a spherical explosion has a single peak (roughly at v_0) followed by a very sharp drop. It is very difficult (and likely even impossible) to produce an energy-velocity profile where high-velocity material carries a significant amount of energy.

As a relativistic jet carves its way through the stellar envelope a double shock (forward–reverse) structure forms at its head (Blandford & Rees 1974; Mészáros & Rees 2001; Matzner 2003; Lazzati & Begelman 2005; Bromberg et al. 2011b). The head propagates with a velocity that is much slower than the jet itself. For typical jet-star parameters seen in GRBs this velocity is mildly relativistic (Zhang et al. 2004). The hot head material forms a cocoon that engulfs and collimates the jet. While the jet propagates in the envelope its energy is dissipated into the cocoon. The jet continues to propagate as long as the engine driving it operates. If it operates long enough it breaks out and powers a GRB. On the way it deposits in the cocoon energy, $E_j = L_j t_{\rm bo}$, where L_j is the jet's luminosity and $t_{\rm bo}$ the breakout time (Bromberg et al. 2011b; Harrison et al. 2018). Otherwise the jet stalls and deposits into the cocoon all its energy, $E_j = L_j T$, where T is the engine operating time. The cocoon contains the stellar mass within a

cone with a half opening angle θ_c (Bromberg et al. 2011b) that is comparable or larger than the opening angle of the original jet, θ_j. The cocoon, which is much hotter than the surrounding matter, expands and breaks out from the star (see Figure 2). At this stage it expands rapidly sideways and engulfs the star (see Figure 2). Its bulk velocity is of order

$$v_c \approx 0.1c\sqrt{E_{j,51.5}/M_{10}\theta_{c,10\circ}^2}. \qquad (1)$$

Clearly some of the cocoon's matter will move at even larger velocities, reaching 0.2–0.3c (see Figure 1).

Regardless of whether or not the jet penetrates the entire star or is choked after crossing a significant fraction of the envelope, the jet deposits a significant amount of energy at the outer layers of the envelope, bringing it to a very high velocity. The resulting velocity profile is very different than that of a spherical explosion. The energy as a function of velocity, $E(v)$, is then the sum of two components: the one that peaks at v_0 and decreases rapidly at higher velocities, and the high-velocity cocoon component that peaks near v_c. The latter reflects the jet properties and it depends on the jet parameters: the energy and the opening angle, as well as the depth at which the jet is choked. An energetic jet that is choked near the surface will produce a high-velocity component that can be clearly identified, possibly even as a second peak. A less-energetic, wider, or a deeply choked jet will give rise to a less-energetic and slower cocoon whose contribution will be weaker and at lower velocities and thus more difficult to separate from the bulk of the SN ejecta.

3. The Cocoon Signature

The cocoon can be identified both by emission and by absorption. Shock breakout emission is the first signature. Given the mildly relativistic velocity, this is a faint burst of gamma-rays with characteristic properties (Nakar & Sari 2012). It might have been the origin of the observed gamma-rays in several of the cases discussed below (Kulkarni et al. 1998; Campana et al. 2006; Bromberg et al. 2011a; Nakar 2015). This is followed by X-rays, and then ultraviolet (UV) and optical (Lazzati et al. 2017; Nakar & Piran 2017; De Colle et al. 2018) that escape from the expanding cocoon when it reaches $\tau \approx c/v$.

The cocoon cooling emission a is UV/blue signal that might be observed if the SN is caught sufficiently early. While relatively bright, detection faces three different obstacles. First, this signal is rather short lived and it has to be caught early enough. Second, it might be hidden by the rising ^{56}Ni decay-driven emission. Third, in cases when a GRB points toward us and the event is caught early on, the brighter GRB afterglow outshines it.

The second signature is very broad absorption features in the SN spectrum that can be observed for a somewhat longer period. During the first few days the cocoon material that has spilled around the star contains some optically thick absorption lines, which due to the high-velocity produce very broad absorption features. After a few days this fast-moving material becomes transparent, the cocoon's very broad absorption lines disappear, and the absorption is dominated by the SN ejecta. As material expands the absorption takes place at lower velocities, therefore a series of spectra taken at different time enables us to determine the velocity profile.
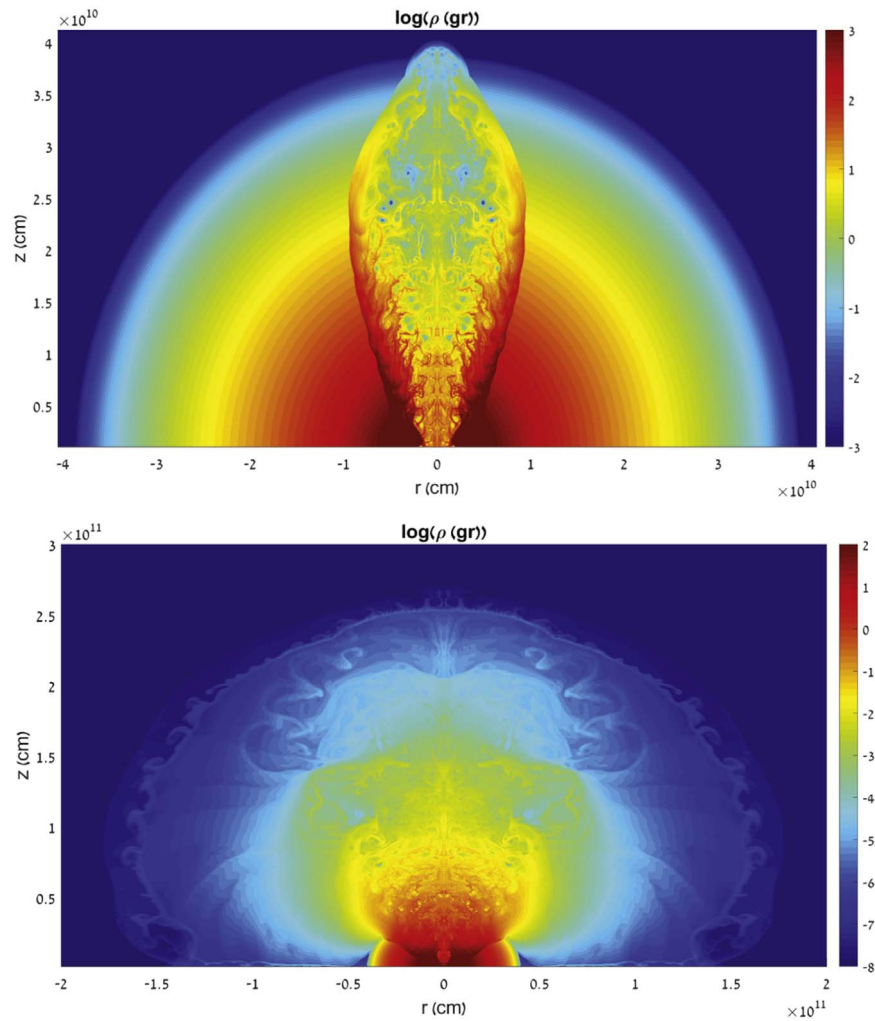
Figure 2. Two snapshots from a relativistic hydrodynamic simulation of a choked relativistic jet done using the code PLUTO (Mignone et al. 2007) (from O. Gottlieb 2019, private communication). The jet, with an opening angle of 8°, is choked when it is halfway through the stellar envelope. At that time the cocoon opening angle is similar to the jet opening angle. At breakout (top panel) the cocoon half opening angle is $\theta_c \approx 20°$. After breakout the cocoon material spills out of the star and spreads (bottom panel). The simulation includes only a jet and does not include the more spherical SN explosion.

4. Observations

An excess of high-velocity material ($\gtrsim 0.1c$) compared to the expectation from a spherical model has been observed in all hydrogen-stripped SNe with available early spectra (see Figure 1 and Table 1). The density profiles, $\rho(v)$, for each SN were obtained from explosion models used to describe the photometric and spectral evolution of each event and are referenced in the various papers (see Table 1). In all of these cases a slowly decreasing density profile with high velocities was required to obtain the observed broad lines (see e.g., for SN1997ef Mazzali et al. 2000). These models then provide $E(v) \equiv \rho v^2/2$.

The prominence of the excess differ from one SNe to another, and so does the confidence that the observations cannot be explained by a spherical explosion.

SN1997ef shows the strongest jet signature (see Figures 1 and 2 of Mazzali et al. 2000 for the early spectra and Figure 8 for the density profile). At low velocities the energy profile fits very well the theoretical model of a spherical explosion of a typical progenitor. However, a well-separated component dominates at $v > 25,000 \, \mathrm{km \, s^{-1}}$. The energy and mass of the fast component, which can be estimated relatively well,

measure the jet energy and put an upper limit on the jet opening angle. A less-pronounced, yet clear, flattening of the energy profile is seen in SN2002ap (at $v \approx 30,000 \, \mathrm{km \, s^{-1}}$) and SN2008D (at $v \approx 17,000 \, \mathrm{km \, s^{-1}}$). The flat energy profile enables a rather robust estimate of the fast component energy, but its mass, which is dominated by material with velocity near the flattening point, cannot be well separated from that of the bulk of the ejecta. SN2003bg exhibit a "bump" in the energy profile at $15,000 < v < 30,000 \, \mathrm{km \, s^{-1}}$. The bump is seen near the peak of the energy distribution and not as a separate component as in SN1997ef, and therefore its identification as jet activity is less secure. Yet, such an energy profile is not expected in a spherical explosion of a conventional progenitor, and jet activity provides a good explanation. Finally, SN1998bw and 2016jca do not show a flattening of the energy profile at high velocities, but they also do not show the expected steepening. At $v > 30,000 \, \mathrm{km \, s^{-1}}$ the energy profiles are significantly shallower than those expected in a regular spherical SN. Thus, while not demonstrating clearly a powerful jet signature these profiles show an excess of fast-moving material suggesting jet activity. At least in SN 2016jca we know that a jet exists as it is associated with a regular LGRB.

Table 1
Properties of the SNe Discussed Here

SN	Type	E_{tot}[a]	M_{ej}[b]	E_j[a]	M_c[b]	θ_c	Comments
1997ef (1)	Ic-BL	20	8	9	0.4	20°	No GRB
1998bw (2)	Ic-BL	50	11	$\gtrsim$2	⋯	⋯	*ll*GRB980425
2002ap (3)	Ic-BL	4	2.5	0.3	⋯	⋯	No GRB
2003bg (4)	IIb	5	4.5	1	0.2	20°	No GRB
2008D (5)	Ib	6	7	1.4	⋯	⋯	X-ray burst
2016jca (6)	Ic-BL	50	10	$\gtrsim$2	⋯	⋯	GRB161219b

Notes. E_{tot} and M_{ej} are the total SN energy and ejected mass. E_j and M_c are the energy and the mass excess of material moving at high velocities over the prediction of a spherical explosion (see Figure 1), and θ_c is the corresponding half opening angle of the cocoon upon breakout. In all SNe, except for SNe 1998bw and 2016jca, the energy of the high-velocity material is only weakly sensitive to the exact spherical model. In SNe 1997ef and 2003bg the inferred mass depends only weakly on the spherical model. In these SNe M_c provides an estimate of θ_c, which in turn puts an upper limit on the jet opening angle. In SNe 1998bw and 2016jca the energy excess at high velocities depends somewhat on the underlying spherical models. Moreover, if this excess is due to cocoon material then most of the cocoon energy may be at velocities where the energy profile is dominated by the bulk of the ejecta, and therefore these E_j values are rough lower limits on the jet energies in these two SNe. Note that all values in the table have been calculated assuming spherical symmetry. As the expanding material is not expected to be fully spherically symmetric, this introduces an uncertainty of a factor of a few in these estimates.
[a] Measured in 10^{51}erg.
[b] Measured in $M_\odot$.
References. 1. Mazzali et al. (2000) 2. Iwamoto et al. (1998) 3. Mazzali et al. (2002) 4. Mazzali et al. (2009) 5. Mazzali et al. (2008) 6. Ashall et al. (2017).

Most interesting is the variety of SN types in which jet signature is detected. These cover almost all types of CCSNe from progenitors that lost all, or most, of their hydrogen envelope. SNe 1997ef and 2002ap are broadline Ic that are not associated with any type of high-energy emission. In particular, SN 2002ap was observed extensively and showed no signs of a relativistic outflow. Radio and X-rays observed several days after the explosion indicate that the velocity of the fastest-moving material in this SNe is $\sim$70,000 km s^{-1} (Björnsson & Fransson 2004). In addition, it shows broad lines only in its early spectra, while the lines in the later spectra (near and after the peak) are relatively narrow, similar to those observed in regular SNe Ic. A jet signature is also seen in the relatively regular type Ib SN2008D. It shows broad lines at early times (produced by cocoon material according to our interpretation), which disappear at later times. SN2008D also shows an early optical component with a luminosity of $\sim$10^{42} erg s^{-1} and a temperature of $\sim$10,000 K (Modjaz et al. 2009), which fits the expected cooling cocoon emission discussed above. If the excess of material at high velocities in SN2003bg is also interpreted as a cocoon material, then jets are active also in SN that lost most, but not all, of their H envelope (type IIb). Finally, we detect a less-pronounced, yet possible, jet signature also in broadline Ic SNe that are associated with LGRBs. SN2016jca is associated with a regular LGRB, in which a jet must have been active. SN1998bw is associated with a low-luminosity GRB980425, whose gamma-rays are fainter by three to four orders of magnitude than in regular LGRBs. Here the observed gamma-rays are most likely a result of a mildly relativistic shock

breakout through an extended envelope (Nakar & Sari 2012; Nakar 2015) and if a jet was active, it was most likely choked. Interestingly, the jet that we infer from the optical spectra carried $\gtrsim$2 × 10^{51} erg, while the gamma-ray emission that preceded SN1998bw carried $\sim$10^{48} erg and its radio emission indicates a mildly relativistic ejecta with $\Gamma \sim 3$ that carried $\sim$10^{49} erg (Kulkarni et al. 1998).

The very broad absorption lines of the fast-moving material can be detected only in very early spectra (see Figures 8–10 in Mazzali et al. 2017). To our knowledge all stripped envelope CCSNe with an early enough spectra show this signature, suggesting that a large fraction of CCSNe harbor such events. However, as the present sample is limited and irregularly sampled we cannot infer the rate and if other types of CCSNe, and in particular superluminous SNe, show this signature as well.

5. Conclusions

We suggest that this energetic fast-moving component is the cocoon that was driven by a relativistic jet. These powerful jets deposit in the cocoons a significant fraction of the explosion energy that is comparable to the one observed in LGRB jets.

Other circumstantial, though less conclusive, evidence supports our inference concerning the existence of jets in SNe. Optical spectropolarimetry of SN2002ap suggests a nonisotropic fast component with energy and velocity similar to those found here (Totani 2003). More generally, double-peaked oxygen nebular lines, implying a significant asphericity, are observed in a large fraction of SNe Ib/c (Mazzali et al. 2005; Maeda et al. 2008; Taubenberger et al. 2009). The appearance of Ni in outer regions (i.e., high velocity) of the SNe provides additional indirect supporting evidence. Clearly a jet that emerges from the inner parts of the core would bring freshly synthesized Ni to the outer regions (Iwamoto et al. 1998; Mazzali et al. 2000, 2002, 2009, 2008; Ashall et al. 2017). Finally, the structure of CCSNe remnants also support jet activity during the SN explosion (Grichener & Soker 2017).

While the jets that we infer do not contain enough energy to drive the SN explosion, they may be the smoking gun of what actually does. First, a fast rotating core is almost certainly required and magnetic fields are also likely to play a major role. Second, this jet activity suggests a relationship between the explosion mechanism of regular type Ib,c CCSNe and the extremely energetic ones associated with GRBs. This puts into question the ability of the popular neutrino-driven mechanism to drives these SNe, and suggests that any model of CCSNe explosion mechanism (at least of type Ib,c) should be able to produce an extremely energetic quasi-spherical explosion accompanied by a narrow and energetic relativistic jet.

The SNe discussed here do not include SNe IIp. However, this does not imply that these SNe do not harbor choked jets. The massive H envelope in this type of SNe is expected to choke not only the jet but also the cocoon, thereby washing out any jet signature from the early spectra. The observation that jets are ubiquitous in SN explosions suggests that the low-metallicity implied from the location of LGRBs is not an essential ingredient for the activity of a central engine. Finally, we note that while the current sample of this kind of SNe is small, upcoming transient searches (Zwicky Transient Facility, *GAIA*, Large Synoptic Survey Telescope, and others) will enable us to detect regularly early SNe spectra. Those will

Piran et al.

reveal the fraction of SNe that harbor jets and will shed new light on SNe engines.

The shocks involved in these hidden jets can be sources to multimessenger signatures. They could be source of high-energy neutrinos observed by IceCube (Aartsen et al. 2017). While these shocks are expected to be radiation dominated, it is possible that a small fraction of the energy dissipated is channeled into high-energy neutrinos (Mészáros & Rees 2001; Xiao & Dai 2014, 2015). If, as we find here, that relativistic jets are common in SNe then their high abundance reduces significantly the required energy output. Furthermore, as these sources are optically thick the Waxman & Bahcall (1999) bound does not apply to them. Interestingly, the hidden jets can also be detectable sources of gravitational radiation. The acceleration of a relativistic jet also produces gravitational radiation (Piran 2002; Birnholtz & Piran 2013). Depending on the parameters, and in particular on the initial Lorentz factor and the duration of the acceleration phase, a hidden jet in a nearby SN taking place at 10 Mpc might be detectable by advanced LIGO.

Note added: While our paper was being refereed Izzo et al. (2019) published early spectra of SN 2017iuk, which is associated with the Gamma-ray burst GRB 171205A. These observations provide strong support to our interpretation of the data.

ORCID iDs

Tsvi Piran ⬤ https://orcid.org/0000-0002-7964-5420
Paolo Mazzali ⬤ https://orcid.org/0000-0001-6876-8284
Elena Pian ⬤ https://orcid.org/0000-0001-8646-4858

References

Aartsen, M. G., Abraham, K., Ackermann, M., et al. 2017, ApJ, 835, 45
Ashall, C., Pian, E., Mazzali, P. A., et al. 2017, arXiv:1702.04339
Baade, W., & Zwicky, F. 1934, PhRv, 46, 76
Birnholtz, O., & Piran, T. 2013, PhRvD, 87, 123007
Bisnovatyi-Kogan, G. S. 1970, AZh, 47, 813
Björnsson, C.-I., & Fransson, C. 2004, ApJ, 605, 823
Blandford, R. D., & Rees, M. J. 1974, MNRAS, 169, 395
Bromberg, O., Nakar, E., & Piran, T. 2011a, ApJL, 739, L55
Bromberg, O., Nakar, E., Piran, T., & Sari, R. 2011b, ApJ, 740, 100
Campana, S., Mangano, V., Blustin, A. J., et al. 2006, Natur, 442, 1008
De Colle, F., Lu, W., Kumar, P., Ramirez-Ruiz, E., & Smoot, G. 2018, MNRAS, 478, 4553
Grichener, A., & Soker, N. 2017, MNRAS, 468, 1226
Harrison, R., Gottlieb, O., & Nakar, E. 2018, MNRAS, 477, 2128
Iwamoto, K., Mazzali, P. A., Nomoto, K., et al. 1998, Natur, 395, 672
Izzo, L., de Ugarte Postigo, A., Maeda, K., et al. 2019, Natur, 565, 324, https://www.nature.com/articles/s41586-018-0826-3
Janka, H.-T. 2012, ARNPS, 62, 407
Kulkarni, S. R., Frail, D. A., Wieringa, M. H., et al. 1998, Natur, 395, 663
Kumar, P., & Zhang, B. 2015, PhR, 561, 1
Lazzati, D., & Begelman, M. C. 2005, ApJ, 629, 903
Lazzati, D., López-Cámara, D., Cantiello, M., et al. 2017, ApJL, 848, L6
LeBlanc, J. M., & Wilson, J. R. 1970, ApJ, 161, 541
Maeda, K., Kawabata, K., Mazzali, P. A., et al. 2008, Sci, 319, 1220
Matzner, C. D. 2003, MNRAS, 345, 575
Matzner, C. D., & McKee, C. F. 1999, ApJ, 510, 379
Mazzali, P. A., Deng, J., Hamuy, M., & Nomoto, K. 2009, ApJ, 703, 1624
Mazzali, P. A., Deng, J., Maeda, K., et al. 2002, ApJL, 572, L61
Mazzali, P. A., Iwamoto, K., & Nomoto, K. 2000, ApJ, 545, 407
Mazzali, P. A., Kawabata, K. S., Maeda, K., et al. 2005, Sci, 308, 1284
Mazzali, P. A., McFadyen, A. I., Woosley, S. E., Pian, E., & Tanaka, M. 2014, MNRAS, 443, 67
Mazzali, P. A., Sauer, D. N., Pian, E., et al. 2017, MNRAS, 469, 2498
Mazzali, P. A., Valenti, S., Della Valle, M., et al. 2008, Sci, 321, 1185
Mészáros, P., & Rees, M. J. 2001, ApJL, 556, L37
Mignone, A., Bodo, G., Massaglia, S., et al. 2007, ApJS, 170, 228
Modjaz, M., Li, W., Butler, N., et al. 2009, ApJ, 702, 226
Nakar, E. 2015, ApJ, 807, 172
Nakar, E., & Piran, T. 2017, ApJ, 834, 28
Nakar, E., & Sari, R. 2012, ApJ, 747, 88
Ostriker, J. P., & Gunn, J. E. 1971, ApJL, 164, L95
Piran, T. 2002, in General Relativity and Gravitation, ed. N. T. Bishop & S. D. Maharaj (Singapore: World Scientific Publishing), 259
Piran, T. 2004, RvMP, 76, 1143
Taubenberger, S., Valenti, S., Benetti, S., et al. 2009, MNRAS, 397, 677
Totani, T. 2003, ApJ, 598, 1151
Waxman, E., & Bahcall, J. 1999, PhRvD, 59, 023002
Woosley, S. E., & Bloom, J. S. 2006, ARA&A, 44, 507
Xiao, D., & Dai, Z. G. 2014, ApJ, 790, 59
Xiao, D., & Dai, Z. G. 2015, ApJ, 805, 137
Zhang, W., Woosley, S. E., & Heger, A. 2004, ApJ, 608, 365